Molecular-dynamics study of liquid rubidium

Raymond D. Mountain
Thermophysics Division, National Bureau of Standards, Washington, D.C. 20234
(Received 3 May 1982; revised manuscript received 12 July 1982)

Molecular dynamics has been used to investigate the properties of supercooled liquid states for a model of liquid rubidium. The energy-temperature relation for the reduced density $n^*=0.95$ for liquid, amorphous solid, and bcc crystal phases is presented along with the pair-correlation function, the self-diffusion coefficient, and the transverse-current correlation as functions of temperature for the liquid. The self-diffusion coefficient is found to vary with temperature in a way which correlates with the temperature evolution of the pair-correlation function. The power spectra of the transverse-current correlation function are used to determine the minimum length required for the decay of fluctuations to be describable by linearized hydrodynamics. This length grows rapidly as the amount of supercooling increases and becomes significantly larger than the dimensions of the cube to which periodic boundary conditions are applied.

I. INTRODUCTION

The results of a molecular-dynamics study of supercooled liquid states at constant density for a model of liquid rubidium are reported in this paper. The characterization of supercooled liquids, i.e., liquids at temperatures lower than the freezing temperature, is one of the more interesting, unresolved topics in liquid state physics.[1] Since a supercooled liquid is not in thermal equilibrium but is, instead, in a stationary or metastable state, a supercooled liquid is sensitive to external disturbances and can be induced to undergo heterogeneous nucleation to the solid phase well before any inherent limit (where homogeneous nucleation occurs) to the amount of supercooling can be reached. If one assumes that such a well defined limit exists, it is natural to inquire into the quantities which determine it and into the mechanisms of homogeneous nucleation.

Broadly speaking, there are two schools of thought concerning the mechanisms. One school assumes the existence of a dynamical mode of the liquid which, at the homogeneous nucleation limit, becomes soft and renders the liquid unstable against the formation of the crystalline phase. These ideas are frequently grouped under the heading spinodal decomposition theories.[2] The other point of view asserts that the onset of homogeneous nucleation is determined by the overall slowing down of processes which occurs as the temperature is lowered so that the lifetime of fluctuations which produce crystal-like local configurations become long enough for the growth of the crystal phase to be the most probable event.[3,4] (This way of thinking accounts for glass formation by further asserting that crystal-like configurations have negligible probability of occurence.[1] Then the only possibility is further slowing down until an amorphous solid is formed.)

It is inherently difficult to perform clean experiments on simple supercooled liquids. Molecular dynamics is an attractive way to explore this subject since all aspects of the structural and dynamical properties of the fluid are, in principle, available for study. There have been a number of molecular-dynamics and Monte Carlo investigations of glass formation in several fluid systems including the widely studied Lennard-Jones fluid. This body of work has been discussed in detail by Angell, *et al.*[4,5] There are limitations on computer simulation investigation of metastable systems due to the small size of the system and the short time intervals which can be studied. Of the two, the time interval appears to pose the more serious problem for the study of metastable states.

The molecular-dynamics results reported here for rubidium do not show evidence for a soft mode instability and do tend to support the idea of "slowing down." The properties examined are the radial distribution function $g_2(r)$, the self-diffusion coefficient D, and the effective coefficient of shear viscosity $\tilde{\eta}(Q,\omega)$ which is associated with transverse momentum current fluctuations. Also, an energy-temperature curve for one density was obtained for the liquid, for the bcc crystal, and for the amorphous solid. This isochore resulted from the determination of the regions of stability of the phases for the time interval readily available during a comput-

er simulation. This time interval is on the order of 10^{-10} s.

The rubidium potential is less harshly repulsive than the Lennard-Jones potential and it is interesting that the temperature dependence of the self-diffusion coefficient of supercooled liquid rubidium is found here to differ significantly from that found for the Lennard-Jones fluid. Also, it is much more difficult to form glassy rubidium than it is to form a glassy Lennard-Jones solid. These are two examples of how rubidium differs from other simple metastable fluids which have been studied by computer simulation. Further discussion of these comparisons is contained in Sec. IV. Note that "rubidium" refers to the model of rubidium studied by molecular dynamics. This model, described in Sec. II, has been found to provide a good description of density fluctuations.[6]

The paper is organized as follows. The molecular-dynamics method and the states studied are discussed in Sec. II. The results for various properties are discussed in Sec. III and a discussion of these results is presented in Sec. IV.

II. MOLECULAR-DYNAMICS CALCULATIONS

The classical equations of motion for 432 interacting Rb particles were integrated using the Beeman algorithm.[7–9] The effective pair potential of Price *et al.*[10] was used to describe the interaction between the Rb ions and was constructed using the parameters listed in Table I of Ref. 11 for a lattice parameter of 5.739 Å. This leads to a reduced density of $n^*=n\sigma^3=0.95$, where n is the number density and $\sigma=4.48$ Å is the smallest zero of the potential. The well depth is $\epsilon=393k_B$, where k_B is Boltzmann's constant. The potential was truncated at 2.03σ. The units of length energy and time were chosen to be σ, ϵ, and

$$\tau=(m\sigma^2/\epsilon)^{1/2}=2.29\times10^{-12}\text{ s},$$

where m is the mass of a Rb atom. The particles were contained in a cube with a side of constant length 7.6896σ and periodic boundary conditions and the minimum image convention were employed when determining the forces, when determining $g_2(r)$, and when integrating the equations of motion. A time step of $\Delta t=0.01\ \tau$ was employed in these calculations. This led to a satisfactory level of energy conservation of a few parts in 10^4.

For each state examined, initial velocities and positions were taken from an earlier fluid or crystal simulation with the velocities scaled so that the desired total energy was achieved. An equilibration period was run to stabilize the system in this new state. For a fluid state, $500\Delta t$ was a sufficient time interval to stabilize the system. For a crystalline state, longer intervals on the order of $2000\Delta t$ were required while amorphous solid states quenched from a fluid required intervals as long as $10\,000\Delta t$ provided nucleation did not occur. The criterion for stability was that the specific heat estimated using the fluctuation theory expression[12,13]

$$\frac{C_v}{k_B}=\frac{3}{2}\left[1-\tfrac{3}{2}N\frac{\langle(\Delta K)^2\rangle}{\langle K^2\rangle}\right]^{-1} \tag{1}$$

be in the range 3–4. Here N is the number of particles (432 in our case), K is the kinetic energy per particle, the angular brackets $\langle\ \rangle$ indicate a time average of the enclosed quantity and $\Delta K=K-\langle K\rangle$. When C_v/k_B determined in this way excedes 4 (or is negative), it is almost certain that the temperature of the system is drifting and that the system is not in a stationary state. Temperature is taken as $T^*=k_BT/\epsilon=\frac{2}{3}\langle K\rangle$.

In this paper we only report results for systems which exhibit stability in the kinetic energy per particle (temperature) during the time interval over which data were taken. For supercooled liquid states, it is essential to observe this stability criterion carefully lest features of nonstationary states enter the results.

The states considered in this paper are indicated by an energy-temperature curve in Fig. 1. The upper branch of the curve represents fluid states to the right of the break and amorphous solid states to the left of the break. The lower branch represents the bcc crystalline states. For this density,

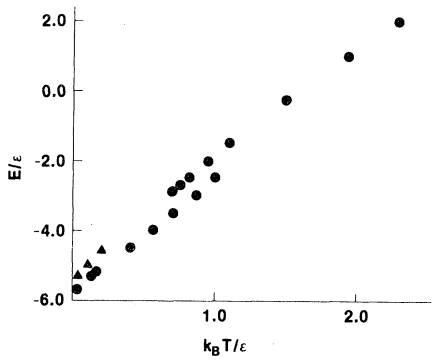

FIG. 1. Energy vs temperature plot for $n^*=0.95$. Upper branch represents fluid states and the lower branch represents bcc crystalline states. ▲ represents amorphous solid states which may be metastable.

$n^*=0.95$, the fluid becomes thermodynamically metastable below $T^*=0.81$ as determined by the thermodynamic argument outlined in Appendix A. The empirical criterion[14,15] that R, the ratio of the amplitude of $g_2(r)$ at the first minimum to the amplitude at the first maximum, equals 0.20 ± 0.01 at freezing places the transition in the interval $0.80<T^*<0.95$. The ratio R is shown as a function of temperature in Fig. 2. The break in the upper branch of Fig. 1 corresponds to a region where the system is unstable against nucleation into the crystalline phase. That is, if a fluid is quenched into that energy-temperature region or if an amorphous solid is heated into that region, the system will spontaneously go over to the bcc phase. The time interval required for this transformation to begin can be quite long (up to $10\,000\Delta t$ for the studies reported here) but once the process starts, it goes to completion within a few hundred Δt. An example of the spontaneous nucleation event is discussed in Appendix B. There the use of an abrupt temperature rise as the indication that nucleation has occurred is elaborated.

The crystalline branch terminates at a temperature where the solid becomes unstable against thermal motion. This is not the melting point as there is no free surface in the system but instead is the limit to the metastability of the superheated crystalline state. For this density, this process occurs for $T^*=1.07$. From earlier Monte Carlo studies on this system, we know that the solid branch bends up toward the fluid branch as this temperature is approached and that C_v becomes quite large.[11]

The preparation of amorphous solid states which are stable is not a simple process. The states represented in Fig. 1 were prepared by repeatedly quenching a fluid until an energy $E=-4.6\epsilon$ was obtained. This configuration was then allowed to evolve at constant energy. Also, after $500\Delta t$, the system was further quenched to $E=-5.0\epsilon$ and also allowed to evolve at constant energy. For both states, the evolution process was followed until the temperature fluctuation stability criterion was satisfied. A stable condition for $E=-5.0\epsilon$ was obtained only after $10\,000\Delta t$, while $6000\Delta t$ was required to stabilize the $E=-4.6\epsilon$ case. The $T=0$ value of $E=-5.294\epsilon$ was obtained by relaxing the stable $E=-5.0\epsilon$ configuration to a local energy minimum.

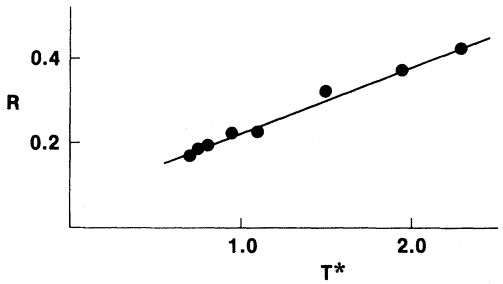

FIG. 2. R, the ratio of the magnitude of $g_2(r)$ at the first minimum to the magnitude of $g_2(r)$ at the first maximum is shown as a function of temperature for the liquid states. Straight line is intended only to guide the eye. Empirical freezing criterion $R=0.20\pm0.01$ places the freezing temperature in the interval $0.80<T^*<0.95$.

A stable amorphous solid was not always obtained using this procedure. The outcome depends in part on the particular liquid configuration quenched. Recall that Hsu and Rahman[16,17] quenched a liquid state to $T^*=0.15$ ($E=-4.8\epsilon$) and the apparently metastable solid went over to the bcc branch after about $8000\Delta t$ (in our time units where $\Delta t=0.01$). The $E=-4.6\epsilon$ state has not been extended beyond $6000\Delta t$ so it may or may not be a metastable state. The $E=-5.0\epsilon$ state has been run for up to $18\,000\Delta t$ without any indication of instability. All of our attempts to produce an amorphous metastable solid state with a 250-particle system have been unsuccessful.

This would suggest that metastable amorphous solid states exist only at quite low temperatures if they exist at all. Certainly, $E=-4.6\epsilon$ is some sort of upper bound on the energy of the metastable solid as heating that state so that the energy increases to -4.3ϵ leads to the formation of the bcc solid. Further research would be needed to clarify this topic. Since our concern here is with the supercooled liquid states, we now concentrate on fluid properties.

The lower limit for the metastable liquid branch lies in the vicinity of $T^*=0.64$ ($E=-3.1\epsilon$). Fluid states quenched to lower energies that lie in the break of the upper branch of Fig. 1 spontaneously go over to the bcc phase after a time interval of a few thousand Δt. The time interval depends on both the way the quench was performed and on the initial configuration quenched.

The case with $E=-3.1\epsilon$ is instructive of the difficulties associated with locating a sharp limit to the metastable branch. In the early phases of this work, several properties were examined for $E=-3.1\epsilon$ with no indication of instability. However, a $6000\Delta t$ run, designed to obtain transverse momentum current correlation functions, exhibited the sort of behavior Hsu and Rahman found in their nucleation studies.[16,17] Although the tempera-

ture showed no drift during the $6000\Delta t$ interval, the mean-square displacement as a function of time showed liquid behavior for the first $4000\Delta t$ and solid behavior for the next $2000\Delta t$. An extension of the run for another $2000\Delta t$ found liquid behavior again. In another run using a different liquid configuration as the starting point for the quench to $E=-3.1\epsilon$, nucleation to the bcc solid occurred readily. From these simulations we conclude that $E=-3.1\epsilon$ lies outside the metastable region. Configurations with $E=-2.9\epsilon(T^*=0.69)$ show no indication of instability and are presumed to be metastable liquid states.

III. RESULTS

A. Pair-correlation function

The variation with temperature of the pair-correlation function $g_2(r)$, is indicated in Fig. 3 where $g_2(r)$ is shown for several temperatures lying in the normal liquid and in the supercooled liquid regions. There are two trends with temperature which should be noted. The first is the shift in position and narrowing of the first peak which occurs as the temperature is lowered. The peak moves to larger values of r and becomes noticeably higher and sharper. The sharpening trend continues down to the instability region and is reflected in the temperature variation of the ratio R shown in Fig. 2. The shift in the position of the first peak stops when $T^*=0.81$ is reached. The other feature is the evolution of the second peak in $g_2(r)$ which is characteristic of the changes which occur with decreasing temperature for $r/\sigma > 1.5$. The amplitude of this peak increases with decreasing temperature while the r values where $g_2(r)=1$ do not vary.

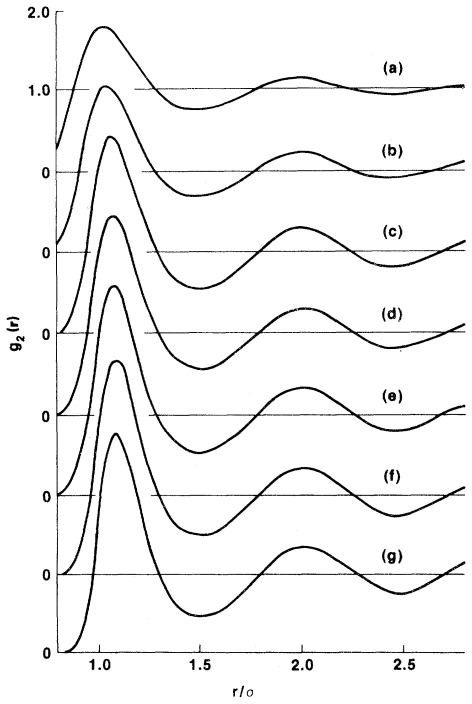

FIG. 3. Pair distribution function $g_2(r)$ is shown for several temperatures: (a) 2.3, (b) 1.5, (c) 1.1, (d) 0.95, (e) 0.81, (f) 0.75, and (g) 0.69. Origins for the curves are vertically offset by unity so the zero level for (f) is the 1.0 level for (g).

B. Self-diffusion coefficient

The self-diffusion coefficient D has been determined using the Einstein relation which states that, for long times, the mean-square displacement of a particle at time t from its position at time zero approaches $6Dt+C$. The constant C is of no interest. The mean-square displacement has been constructed for several fluid states using time intervals of $100\Delta t$ with 20 distinct time origins. A linear increase with time sets in by $50\Delta t$. The self-diffusion coefficients deduced from the slopes of plots of mean-square displacement versus time are plotted in Fig. 4 as a function of $1/T^*$. It is evident from this plot that the temperature dependence of the self-diffusion coefficient changes when the supercooled region is entered.

Recently, this sort of temperature dependence was observed in a molecular-dynamics study of the diffusion of sodium ions in a silicate glass.[18] It was found that the temperature dependence of the diffusion coefficient varied with the rate at which the glass was quenched. In order to see if the present results might also be quench rate dependent, the following test was performed. A liquid at $E=-1.0\epsilon$ was prepared and stabilized. The resulting configuration served as the starting point for three separate quenches to $E=-2.7\epsilon$. In these three runs, the particle velocities were scaled at each step by 0.9, 0.99, and 0.999, respectively, until $E=-2.7\epsilon$ was reached. The system then evolved at constant energy until the temperature stabilized. Then a $2000\Delta t$ run was made to determine D. The results were stable, independent of quench rate, and agreed with those of an $8000\Delta t$ run described in Sec. III D.

Some aspect of the diffusion process changes as the temperature is lowered into the supercooled region. If one thinks in terms of activated processes,

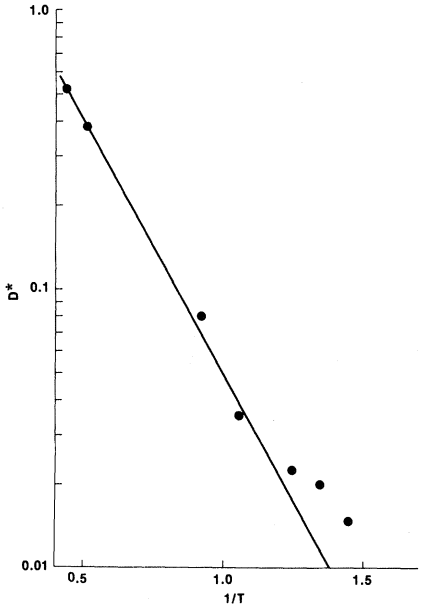

FIG. 4. Reduced self-diffusion coefficient D^* as a function of $1/T^*$. Straight line emphasizes the change in the temperature dependence of D^* as the supercooled region is entered. $D^*=1$ corresponds to $D=8.76\times10^{-4}$ cm^2/s.

the barrier to diffusion is lower in the supercooled region than in the higher-temperature region. (Parenthetically, we note that this type of temperature dependence is observed for diffusion in crystals with the Fluorite structure and is associated with a change in diffusion mechanism.[19]) The self-diffusion coefficients of supercooled Lennard-Jones and inverse 12th power potential liquids show different temperature dependence, albeit at constant pressure rather than at constant density.[20] For these systems, the barrier to diffusion is higher in the strongly supercooled region than it is in the normal liquid region. We shall examine this interesting situation further in Sec. IV.

C. Transverse-current correlations

The power spectra of transverse-current correlation functions[21,22] provide an indication of how the system responds to shear disturbances with wave vector Q and frequency ω. Since supercooling refers to a global rather than a local condition, it is reasonable to expect that the response of a supercooled liquid to short-wavelength and/or high-frequency disturbances will not be sensitive to the degree of supercooling while the response to long-wavelength, low-frequency disturbances will be sensitive to the state of the system. The results described in the following paragraphs are consistent with this viewpoint.

The transverse-current density is

$$\vec{J}_T(Q,t)=\frac{1}{\sqrt{N}}\sum_j \vec{V}_j^T(t)\exp[i\vec{Q}\cdot\vec{r}_j(t)] , \tag{2}$$

where $\vec{V}_j^T$ is that part of $\vec{V}_j$ which is perpendicular to $\vec{Q}$. The transverse-current correlation function is

$$C_T(Q,t)=\langle \vec{J}_T(Q,t+\tau)\cdot\vec{J}_T(-Q,\tau)\rangle . \tag{3}$$

The Cartesian components of the wave vector $\vec{Q}$ satisfy

$$Q_n=\frac{2\pi}{L}n , \tag{4}$$

where L is the length of the side of the periodic cube and n is an integer. In this way, the periodic boundary conditions are satisfied. For these calculations the wave vectors were chosen to lie along the x, y, and z edges of the cube with $n=1,2,\ldots,12$. The results for the three directions were averaged. The time origins τ were separated by $10\Delta t$ and a total of 6000 time steps were employed. $C(Q,t)$ was truncated at $200\Delta t$. The averages include both polarizations for each wave vector $\vec{Q}$ so a total of six quantities go into the average for each time origin.

It is useful to write $C_T(Q,t)$ as a sum of a single-particle term and of a pair term, namely,

$$C_T(Q,t)=\frac{1}{N}\left\langle\sum_j \vec{V}_j^T(t)\cdot\vec{V}_j^T(0)\exp\{i\vec{Q}\cdot[\vec{r}_j(t)-\vec{r}_j(0)]\}+\sum_{j\neq k}\vec{V}_j^T(t)\cdot\vec{V}_k^T(0)\exp\{i\vec{Q}\cdot[\vec{r}_j(t)-\vec{r}_k(0)]\}\right\rangle . \tag{5}$$

For the Q's of interest here, most of the time dependence of the single-particle term is due to changes in the velocity of a particle rather than due to changes in position. So, if the normalized velocity autocorrelation function $\psi(t)$ were to be subtracted from $C_T(Q,t)/C_T(Q,0)$, the result would approximate the normalized second term in Eq. (5). The result of doing this is displayed in Fig. 5 for the $T^*=0.75$ state. $\psi(t)$ is shown in Fig. 6. These results are not specific to supercooled liquids but ap-

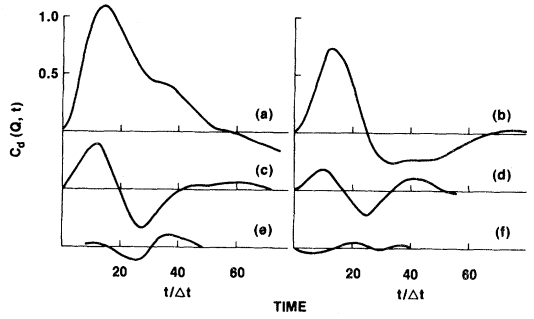

FIG. 5. Distinct part of the transverse-current correlation functions are shown as functions of time for the $T^*=0.75$ state. $C_d(Q,t)=C_T(Q,t)/C_T(Q,t)-\psi(t)$. Parts (a)–(f) are for $Q_1,\ldots,Q_6$, respectively.

pear to be a general feature of transverse-current correlations in liquids. Qualitatively similar results may be obtained using the tabulated values for $\psi(t)$ and $C_T(Q,t)$ found in Ref. 23 for several liquid states.

For small Q's, the collective parts are large and longer lived than the single-particle part. As Q increases, the collective part becomes less pronounced and, for $Q>Q_5$, become insignificant for time intervals longer than the time required for a particle to undergo a velocity reversing interaction. This trend is consistent with the generally observed feature that the dispersion relation for transverse-current modes saturates at moderate values of Q. This saturation reflects the dominance of the single-particle part of the correlation function for larger Q values. For this reason, we focus our attention on the smaller Q's, specifically, $Q<Q_5$.

It is the small Q, small ω portions of

$$\tilde{C}_T(Q,\omega)=\int_0^\infty dt\, C_T(Q,t)\exp(i\omega t) \tag{6}$$

which exhibit significant changes as the temperature is lowered. These changes are illustrated in Fig. 7 for $\mathrm{Re}\tilde{C}_T(Q_1,\omega)$. The spectra for $\omega\geq 30\Delta\omega$ are effectively temperature independent.

The growth with decreasing temperature of the low-frequency dip in $\mathrm{Re}\tilde{C}_T(Q,\omega)$ is a reflection of the increase of the shear viscosity of the liquid. A wave-vector and frequency-dependent shear-viscosity coefficient $\tilde{\eta}(Q,\omega)$ is related to the transverse-current correlations by

$$\frac{\tilde{C}(Q,\omega)}{C(Q,t=0)}=[-i\omega+Q^2\tilde{\eta}(Q,\omega)/\rho]^{-1}, \tag{7}$$

where ρ is the mass density.[22,24,25] In this formulation $Q^2\tilde{\eta}(Q,\omega)/\rho$ is the Fourier-Laplace transform of the memory function for the transverse-current correlation function. The arguments used to derive the equations of generalized hydrodynamics indicate that the long-wavelength, low-frequency limit of $\tilde{\eta}$ is the coefficient of shear viscosity.[24–25] Equation (7) has been solved for $\tilde{\eta}$ and the results for $T^*=0.81$ and $T^*=0.69$ are shown in Fig. 8. As the temperature is lowered, $\mathrm{Re}\tilde{\eta}(Q,\omega)$ develops a low-frequency peak which becomes more pronounced at small Q's while the broad maximum in $\mathrm{Im}\tilde{\eta}(Q,\omega)$ becomes sharper and moves to lower frequency. For frequencies greater than $20\Delta\omega$, the results are uninteresting in that there is very little, if any, temperature dependence.

The trends in $\tilde{\eta}(Q,\omega)$ with increasing temperature are reliable although the explicit values contain a considerable uncertainty because the process of inverting Eq. (7) to obtain $\tilde{\eta}(Q,\omega)$ is quite sensitive to any noise in $\tilde{C}_T(Q,\omega)$. It was for just this reason that the relatively long runs were made.

Another way of considering the enhancement of dynamical correlations is to examine the hydrodynamic length l_t discussed by Jacucci and

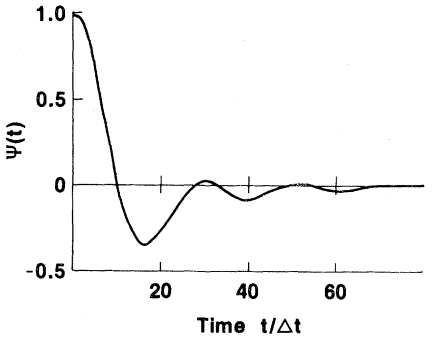

FIG. 6. Normalized, single-particle velocity time correlation function for $T^*=0.75$ is shown as a function of time.

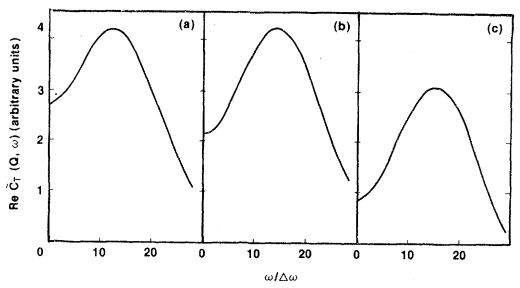

FIG. 7. $\mathrm{Re}\tilde{C}_T(Q,\omega)$ is shown as a function of frequency for (a) $T^*=0.81$, (b) $T^*=0.75$, and (c) $T^*=0.69$. $\Delta\omega=0.153/\tau$.

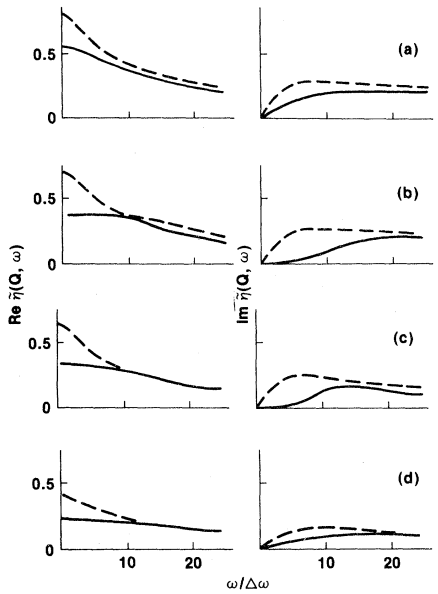

FIG. 8. Effective Q- and ω-dependent shear viscosity $\tilde{\eta}(Q,\omega)$ is shown in arbitrary units as a function of frequency for $T^*=0.81$ (solid curves) and $T^*=0.69$ (dashed curves) for (a) Q_1, (b) Q_2, (c) Q_3, and (d) Q_4. Re$\tilde{\eta}$ is shown in the left column and Im$\tilde{\eta}$ is shown in the right column. $\Delta\omega=0.153/\tau$.

McDonald.[26] In the long-wavelength limit ($Q\rightarrow 0$), the transverse-current correlation function decays exponentially in time and Re$\tilde{C}_T(Q,\omega)$ has its maximum, for a given Q, at $\omega=0$. The hydrodynamic description of fluctuations is limited to wave vectors such that Re$\tilde{C}_T(Q,\omega)$ has a maximum only at $\omega=0$. An upper limit for the largest wave vector for which hydrodynamics applies may be determined by plotting the frequency of the maximum in Re$\tilde{C}_T(Q,\omega)$ as a function of Q and then extrapolating to q_t, the zero frequency intercept. The resulting hydrodynamic length

$$l_t=2\pi/q_t \tag{8}$$

is a measure of the spatial extent of transverse dynamical correlations. This length is shown for five temperatures in Fig. 9. The two high-temperature points were obtained using the transverse-current correlation functions reported in Ref. 23.

The results for $\tilde{\eta}(Q,\omega)$ and for l_t indicate that both the range and the lifetime of the dynamical correlations associated with the transverse momentum current fluctuations increase significantly with the amount of supercooling.

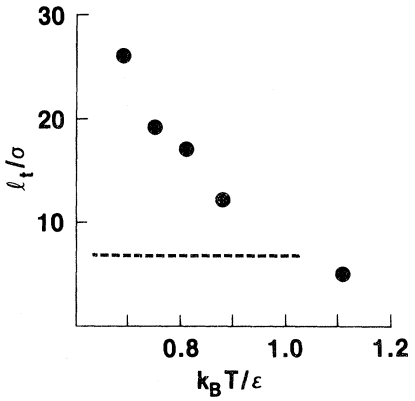

FIG. 9. Hydrodynamic length l_t as a function of temperature for liquid rubidium. Horizontal dashed line indicates the size of the cube to which periodic boundary conditions are applied.

IV. DISCUSSION

The molecular-dynamics results described in Sec. III show interesting variations with temperature of some properties of supercooled rubidium. First we examine the changes in the local structure of the liquid as reflected in the pair distribution function $g_2(r)$.

There are two types of changes in $g_2(r)$ which occur as the temperature is lowered. There is a "sharpening" of the structure which goes on in both equilibrium and supercooled liquid states. There is also evolution of the structure in the form of a shift in the position of the first maximum of $g_2(r)$ to larger r values. This occurs in the equilibrium liquid but is not perceptible in the supercooled liquid. These trends are evident in Fig. 10 where

$$\Delta g=g_2(T^*,r)-g_2(0.81,r)$$

is shown for $T^*=1.1$ (solid curve) and $T^*=0.69$ (dashed curve). Recall that $T^*=0.81$ is close to the freezing temperature while $T^*=1.1$ is an equilibrium state and $T^*=0.69$ is close to the nucleation instability region. The vertical line through the peak of $g_2(0.81,r)$ in Fig. 10 emphasizes the point that the position of that peak has stopped moving in the supercooled liquid.

The pair distribution function represents the average environment of a particle. In the supercooled region, the near-neighbor environment becomes more sharply defined in space but does not shift its position as it does in the equilibrium liquid. That is to say, the local environment stops evolving (in the sense of a peak shift) once the freezing tem-

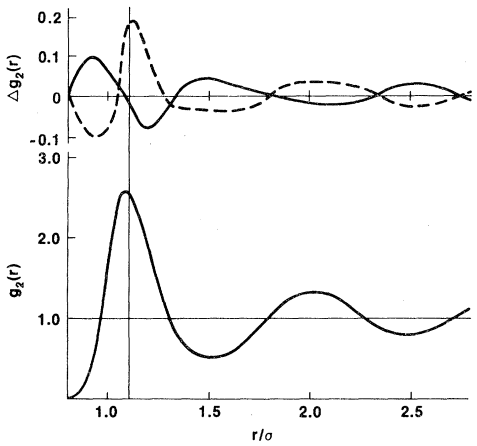

FIG. 10. Change in $g_2(r)$ with changing temperatures is shown relative $g_2(r)$ for $T^*=0.81$ (lower curve) as $\Delta g_2(r)=g_2(T^*,r)-g_2(\Delta 0.81,r)$. Solid curve is Δg_2 for $T^*=1.1$ and the dashed curve for $T^*=0.69$.

perature is reached and in the supercooled region this fully developed liquid structure can only become more sharply defined until crystallization intervenes.

With this information in hand, the temperature dependence of the self-diffusion coefficient may be better appreciated. We have seen that, in the equilibrium liquid, the local environment through which a particle diffuses is evolving as well as becoming more sharply localized as the temperature decreases. In the supercooled liquid, only further sharpening occurs. The saturation of the structure means that self-diffusion occurs in similar environments for supercooled states of differing temperature. As a result, the temperature dependence of D is different in the two regions.

This is to be compared with the high density Lennard-Jones liquid where, for a range of equilibrium liquid states, only the sharpening of the structure of $g_2(r)$ takes place. This may be seen by examining Fig. 11, where $g_2(r)$ is shown for a series of temperatures for $n^*=0.85$ which is close to the triple point density.[27] The freezing temperature is $T^*=0.71$. The Lennard-Jones potential is more strongly repulsive than the rubidium potential so it is not surprising that the evolution of the Lennard-Jones liquid structure is completed at lower densities and at higher temperatures than it is for rubidium.

In terms of the discussion of the relationship of the self-diffusion coefficient to $g_2(r)$, we would expect no sudden change in the temperature dependence of D for the Lennard-Jones liquid. This is indeed what happens as shown in Fig. 12 where D^*

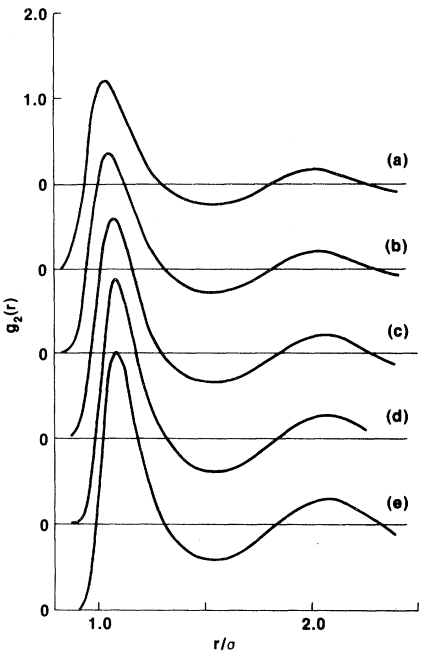

FIG. 11. Pair distribution functions for the Lennard-Jones fluid at a density of $n^*=0.85$ are shown for several temperatures: (a) $T^*=2.888$, (b) $T^*=2.202$, (c) $T^*=1.273$, (d) $T^*=0.88$, (e) $T^*=0.719$. These curves were prepared using data from Ref. 28.

vs T^* is displayed for rubidium ($n^*=0.95$) and for the Lennard-Jones ($n^*=0.85$).[28]

Now let us consider briefly the dynamical correlations present in supercooled liquid rubidium. The

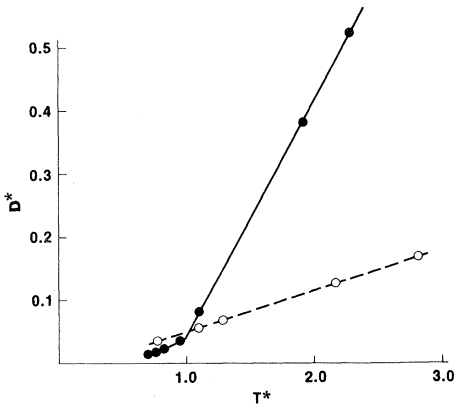

FIG. 12. Self-diffusion coefficients for the Lennard-Jones fluid at $n^*=0.85$ (dashed line) and of rubidium (solid line) as a function of temperature. Lennard-Jones values were taken from Ref. 28 and were multiplied by $\sqrt{48}$ so that both sets of values were reduced in the same way.

transverse-current correlations are significantly enhanced in the supercooled region. The dispersion relation for the propagating transverse mode was used to determine the lower limit for the wavelength of fluctuations whose decay can be described by linearized hydrodynamics. This limiting length was found to increase significantly with decreasing temperature and to be larger than the size of the cube to which periodic boundary conditions are applied. This growth in the spatial extent of the correlation of transverse-current fluctuations is reflected in the increase in $\tilde{\eta}(Q,\omega)$ in the small Q and ω region. It also means that one would have to go to significantly larger systems before the long-wavelength, low-frequency limit could be taken for supercooled liquid rubidium.

ACKNOWLEDGMENT

I wish to thank Ramesh Shukla for providing the lattice-dynamics calculations of the entropy used in Appendix B.

APPENDIX A

The thermodynamic condition for the coexistence of the solid and liquid phases is that the Gibbs free energy $G(P,T)$ of the two phases be equal:

$$G_l(P,T)=G_s(P,T)\ . \tag{A1}$$

This condition has been used to determine the freezing temperature for the $n^*=0.95$ isochore of liquid rubidium. For this purpose, the model potential was assumed to be density independent so the resulting freezing temperature $T^*=0.81$ applies only to this model, not to the substance rubidium.

The entropy for the solid was obtained using lattice dynamics in the quasiharmonic approximation[29] for three temperatures for $n^*=0.95$.[30] Entropies for other temperatures and densities were obtained by integrating

$$dS=\frac{C_v}{T}dT+\left[\frac{\partial P}{\partial T}\right]_v dV \tag{A2}$$

along an appropriate thermodynamic path using molecular dynamics to determine the thermal properties.

The entropy for the liquid was obtained by integrating Eq. (A2) along a path from the ideal gas to the liquid. This path started from $n^*=0.1$ and $T^*=6.0$, where the entropy for the ideal gas plus

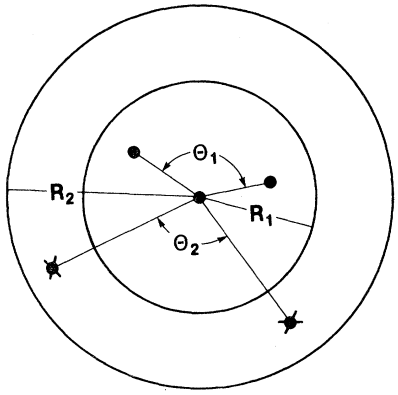

FIG. 13. First neighbors (●) of a particle located at the origin are defined to lie within a sphere of radius R_1 and the second neighbors (✱) are defined to lie within a spherical shell of inner radius R_1 and outer radius R_2. R_1 is taken to be halfway between the first and second neighbors on a bcc lattice and R_2 is the position of the first minimum of $g_2(r)$ in the liquid. Distribution of the cosines of the angles θ_1,θ_2 provide a three-body characterization of the local structure of the system.

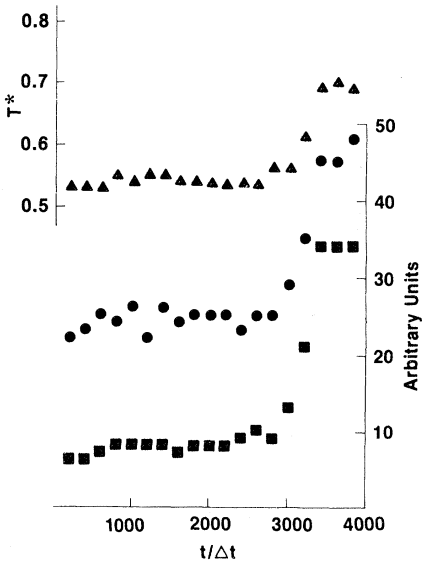

FIG. 14. Evolution of the temperature (▲) and the $\mu=-1$ value of the distributions of the cosines of neighbor angles for first (●) and second (■) neighbors during a quench experiment is shown. Final temperature is that of the equilibrium solid. Scatter of the points is indicative of the short-time fluctuations in local order since each distribution point represents one "snapshot" of the system. Distributions have the same, arbitrary normalization and have a resolution of 0.04 in $\cos\theta$.

second virial coefficient contribution were taken as the reference state. The path followed $T^*=6.0$ to $n^*=0.95$ and then followed $n^*=0.95$ down to $T^*=0.6$.

The Gibbs free energies

$$G=E-TS+PV$$

for the two phases were constructed and Eq. (A1) was satisfied for

$$T^*=0.81\pm0.01,\quad P^*=5.9\pm0.05\ ,$$

$$n_l^*=0.95,\quad n_s^*=0.98\pm0.005\ .$$

The entropy and volume differences of the liquid and solid imply a melting curve with slope of 59 bar/K. This is to be compared with the experimental value[31] for Rb of 50 bar/K.

APPENDIX B

Nucleation of the crystalline state from a fluid state quenched into the thermally unstable region (the gap in the upper branch of Fig. 1) has been studied by Hsu and Rahman.[16,17] The onset of the nucleation process is signaled by an abrupt rise in the temperature of the system. At the same time, the three-body correlations for both first-neighbor and second-neighbor sets undergo changes from fluid to crystalline forms. The sets of first and second neighbors are defined in the caption for Fig. 13. The signature of the crystal is a sharp peaking in the distribution of μ, the cosine of the angle made by the neighbors, around $\mu=-1$ for both sets.[16,17,32]

Typical results for the evolution of the temperature and of the $\mu=-1$ value of the cosine distributions during a quench are displayed in Fig. 14. The μ distributions were sampled every $200\Delta t$ following a quench from $T^*=0.74$ to $T^*=0.53$ and the temperatures are averaged over $20\Delta t$. The changes in the μ distributions coincide with the change in the temperature indicating that the temperature rise is a diagnostic for the nucleation of the solid phase. Temperature rise is the diagnostic employed in this paper to monitor the stability of the system.

[1]J. Wong and C. A. Angell, *Glass: Structure by Spectroscopy* (Dekker, New York, 1976), Chap. 1.

[2]W. Klein and A. C. Brown, J. Chem. Phys. 74, 6960 (1981).

[3]D. Turnbull and J. C. Fisher, J. Chem. Phys. 17, 71 (1949).

[4]C. A. Angell, J. H. R. Clarke, and L. V. Woodcock, *Advances in Chemical Physics, Vol. 48,* edited by I. Prigogine and S. A. Rice (Wiley, New York, 1981), pp. 397–453.

[5]C. A. Angell, Ann. N. Y. Acad. Sci. 371, 136 (1981).

[6]A. Rahman, Phys. Rev. Lett. 32, 52 (1974); Phys. Rev. A 9, 1667 (1974).

[7]P. Schofield, Comput. Phys. Comm. 5, 17 (1973).

[8]M. J. L. Sangster and M. Dixon, Adv. Phys. 25, 247 (1976).

[9]D. Beeman, J. Comput. Phys. 20, 130 (1976).

[10]D. L. Price, K. S. Singwi, and M. P. Tosi, Phys. Rev. B 2, 2983 (1976).

[11]R. A. MacDonald, R. D. Mountain, and R. C. Shukla, Phys. Rev. B 20, 4012 (1979).

[12]J. L. Lebowitz, J. K. Percus, and L. Verlet, Phys. Rev. 153, 250 (1967).

[13]P. S. Y. Cheung, Mol. Phys. 33, 519 (1977).

[14]H. J. Raveche, R. D. Mountain, and W. B. Streett, J. Chem. Phys. 61, 1970 (1974).

[15]F. F. Abraham, J. Chem. Phys. 72, 359 (1980).

[16]C. S. Hsu and A. Rahman, J. Chem. Phys. 70, 5234 (1979).

[17]C. S. Hsu and A. Rahman, J. Chem. Phys. 71, 4974 (1979).

[18]T. F. Soules and R. F. Busbey, J. Chem. Phys. 75, 969 (1981).

[19]J. M. Oberschmidt and D. Lazarus, *Fast Ion Transport in Solids,* edited by P. Vashishta, J. N. Mundy, and G. K. Shenoy (North-Holland, New York, 1979), pp. 691–694.

[20]J. H. R. Clarke, J. Chem. Soc. Faraday Trans. 2 75, 1371 (1979).

[21]A. Rahman, *Neutron Inelastic Scattering, Vol. 1* (IAEA, Vienna, 1968), p. 561.

[22]D. Levesque, L. Verlet, and J. Kurkijarvi, Phys. Rev. A 7, 1690 (1973).

[23]R. D. Mountain and S. W. Haan, J. Res. Natl. Bur. Stand. 84, 439 (1979).

[24]D. J. Evans, Phys. Rev. A 23, 2622 (1981).

[25]R. D. Mountain, Adv. Mol. Relaxation Processes 9, 225 (1977).

[26]G. Jacucci and I. R. McDonald, *Liquid & Amorphous Metals,* edited by E. Lüscher and H. Coufal (Sijthoff & Noordhoff, Alphen aan den Rijn, The Netherlands, 1980), pp. 143–157.

[27]L. Verlet, Phys. Rev. 165, 201 (1968).

[28]D. Levesque and L. Verlet, Phys. Rev. A 2, 2514 (1970).

[29]H. R. Glyde and M. L. Klein, CRC Crit. Rev. Solid State Sci. 2, 181 (1971).

[30]R. C. Shukla (private communication).

[31]S. B. Babb, Jr., Rev. Mod. Phys. 35, 400 (1963).

[32]V. A. Poluchin, M. M. Dzugutov, V. F. Uchov, and N. A. Vatolin, J. Phys. (Paris) 41, C8-284 (1980).